Measurement of the Ground State Spin and Parity of Al22 Disfavors Halo Formation

Measurement of the Ground State Spin and Parity of ^{22}Al Disfavors Halo Formation

E. A. M. Jensen,[1,2,*] J. S. Nielsen,[1] B. S. O. Johansson,[1] A. Adams,[3,4] J. Dopfer,[3,4] C. S. Sumithrarachchi,[4] L. J. Sun,[4] L. E. Weghorn,[3,4] T. Wheeler,[3,4] C. Wrede,[3,4] M. J. G. Borge,[5] O. Tengblad,[5] M. Madurga,[6] B. Jonson,[2] K. Riisager,[1] and H. O. U. Fynbo[1]

[1]*Institut for Fysik & Astronomi, Aarhus Universitet, Aarhus, 8000, Denmark*
[2]*Institutionen för Fysik & Astronomi, Chalmers Tekniska Högskola, 412 96, Göteborg, Sweden*
[3]*Department of Physics and Astronomy, Michigan State University, East Lansing, Michigan 48824, USA*
[4]*Facility for Rare Isotope Beams, Michigan State University, East Lansing, Michigan 48824, USA*
[5]*Instituto de Estructura de la Materia, CSIC, Madrid, 28006, Spain*
[6]*Department of Physics and Astronomy, University of Tennessee, Knoxville, Tennessee 37996, USA*

(Received 8 January 2026; revised 20 March 2026; accepted 27 April 2026; published 20 May 2026)

We report the decisive resolution of the ground state spin and parity of the proton–drip line nucleus ^{22}Al, a prime candidate for a proton halo. The resolution stems from the first β-delayed charged particle emission experiment in the gas stopping area at the Facility for Rare Isotope Beams (FRIB), leveraging high-intensity, low-energy beams extracted from the Advanced Cryogenic Gas Stopper (ACGS). The pristine beam quality from FRIB and the ACGS enabled a sensitive particle identification technique using thin silicon detectors, allowing for the suppression of the dominant proton background and the first observation of the weak β-delayed α transition from the isobaric analog state in ^{22}Mg to the ^{18}Ne ground state. This observation uniquely fixes the ^{22}Al ground state as 4^+. The valence proton is confined by a dominant d-wave centrifugal barrier which, combined with the Coulomb repulsion, hinders the tunneling required for halo formation despite the exceptionally low proton separation energy of ^{22}Al.

DOI: 10.1103/3lpm-sy41

Near the limits of nuclear stability, the classical picture of the nucleus as a compact liquid drop breaks down, giving rise to the nuclear "halo." This exotic structure emerges in loosely bound systems where a vanishing separation energy allows valence nucleons to tunnel far into the classically forbidden region. The resulting spatially extended wave function creates a unique state of dilute nuclear matter that defies standard geometric scaling laws. The nuclear volume tends to scale with the nuclear mass number A, but for halo nuclei, the nuclear matter radius $R \sim A^{1/3}$ can be as large as would be expected for a nuclide composed of 4–5 times as many nucleons; an example of such a case being the nuclear matter radius of ^{11}Li of approximately $R = 3.5$ fm—the same as that of ^{48}Ca [1]. Halo nuclei are rare and serve as distinct test beds for quantum phenomena at the edge of unbinding.

While weak binding is a necessary condition for halo formation, it is not sufficient; the quantum tunneling required to sustain a halo is critically sensitive to the confining potential barriers [2,3]. For a halo to develop, the valence nucleon must not be inhibited by a high potential barrier. Consequently, the orbital angular momentum ℓ plays a decisive role. The centrifugal barrier, proportional to $\ell(\ell+1)$, strongly suppresses the tunneling of nucleons in high-ℓ orbitals, effectively confining the wave function to the nuclear core. Therefore, halos are predominantly associated with s waves ($\ell = 0$) or occasionally p waves ($\ell = 1$). This structural fragility is further compounded in proton-rich nuclei by the Coulomb barrier. Unlike neutrons, which can form halos relatively easily in light nuclei (such as ^{11}Li or ^{11}Be), for loosely bound protons the outer tail will be quenched by the repulsive long-range Coulomb potential. As a result, genuine proton halos are rare and remain a subject of intense debate [4–7].

Proton halos in the sd shell have been envisaged since [8], often in light isotopes of Si and P. Recently, much interest has been given to the lightest bound Al isotope, ^{22}Al. The recent interest started with the observation [9] of an asymmetry between the β decays into the lowest excited 1^+ states in ^{22}Al and its mirror nucleus ^{22}F that was attributed to a proton halo structure. Two detailed theory papers [6,10] do not support this conclusion, in particular not for the ground state, but acknowledge the incomplete experimental situation that has been partially alleviated by recent mass measurements [11,12] which have established

*Contact author: erik.jensen@chalmers.se

the proton separation energy of ^{22}Al to be $S_p = 100.3(8)$ keV [13].

The realization of a halo structure depends entirely on the quantum numbers of the valence nucleon, which dictate the height of the centrifugal barrier. The structure of ^{22}Al can be modeled as a valence proton coupled to a ^{21}Mg$(5/2^+)$ core, but the spin and parity J^π of the ^{22}Al ground state have remained ambiguous, with experimental evidence and theoretical models oscillating between a 3^+ and a 4^+ assignment, as discussed below. This distinction is the primary determining factor for the existence of a halo. A $J^\pi = 3^+$ assignment may allow the valence proton to occupy an $s_{1/2}$ orbital ($\ell = 0$) relative to the core, facing no centrifugal barrier and allowing for the possible formation of an extended proton halo. Conversely, a $J^\pi = 4^+$ assignment places the proton in a $d_{5/2}$ orbital ($\ell = 2$), where the combined centrifugal and Coulomb barriers would confine the proton, resulting in a more standard nuclear structure.

The interest in ^{22}Al is not only due to its potential halo nature, but also due to it being the lightest precursor to β-delayed 2-proton emission [14]. The discovery of β-delayed 2-proton emission was made in the early 1980s [15,16] from ^{22}Al via the isobaric analog state (IAS) in ^{22}Mg. After this discovery was made, the question of whether this decay mode could proceed via direct "^{2}He" emission, as opposed to sequential "proton-proton" emission, was studied theoretically [17]. Apart from the halo nature of ^{22}Al, its ground state spin and parity are also of importance in the context of β-delayed 2-proton emission, since they have implications for the confining potentials which the two protons penetrate during the decay—either sequentially or directly—and as to how well the nuclear structure accommodates one form of decay over the other.

The structural interpretation of ^{22}Al is informed by knowledge from its mirror nucleus ^{22}F, which decays to the stable and well-characterized [18] nuclide ^{22}Ne. Under strict isospin symmetry, the ground state of ^{22}Al has the same spin and parity as the ground state of ^{22}F. Together with ^{22}Mg, ^{22}Na, and ^{22}Ne, these nuclides constitute an isospin $T = 2$ quintet. While the β-decay strength from ^{22}F to excited states in ^{22}Ne restricts the ^{22}F ground state to an even parity and a spin of $J = 3$ or 4 [19], a precise assignment remains elusive. This is in part due to the presence of a first excited state in ^{22}F at just 72 keV. The deexcitation of this state to the ground state is found in [20] to change the spin by one unit and is assigned 3^+, assuming the ground state of ^{22}F is 4^+. A study of the ^{21}F$(d, p)^{22}$F reaction in inverse kinematics has found that the ground and first excited states in ^{22}F, in unison, are dominated by $d_{5/2}$ single-neutron strength [21]. This implies that the ground state of ^{22}F, with a tentative $J^\pi = (3, 4)^+$ assignment, is associated with an $\ell = 2$ coupling of the valence neutron to the ^{21}F core, regardless of the spin of ^{22}F. In the same study, the observation of predominant $d_{5/2}$ single-neutron strength in ^{22}F is shown to agree very well with the results of sd-shell model calculations [22].

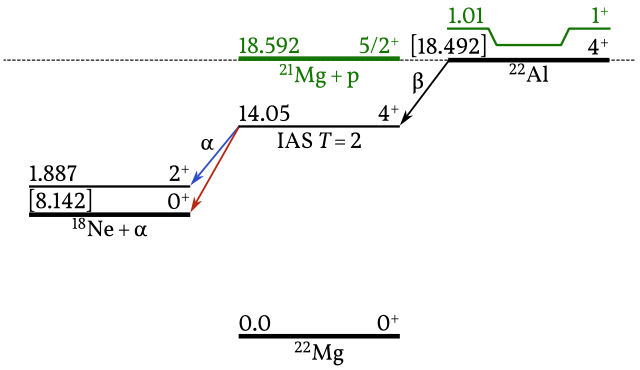

FIG. 1. Decay scheme for the β-delayed α emission of ^{22}Al. The newly observed transition to the ^{18}Ne ground state is highlighted in red. The mass and proton separation energy of ^{22}Al are adopted from [11], and the IAS energy is derived from our measured β-delayed proton spectrum. Other level parameters are adopted from [9,26,27]. The 1.01 MeV 1^+ state in ^{22}Al is the lowest-lying known excited state, and is particle unbound. Its energy is recalculated, based on the new mass measurement in [11], increasing it from 0.91 MeV reported in [9].

What is clear, based on the available literature on the $T = 2$ quintet, is that the two lowest-lying states in ^{22}F are 3^+ and 4^+; two 3^+ states in such close proximity is highly unlikely. It is, however, unclear which of the two states has the lowest energy in ^{22}F. In the proton-rich ^{22}Al, the Thomas-Ehrman shift—driven by the spatial extension of the unbound proton wave function—could lower the energy of the analog 3^+ state, which could, in turn, be associated with a low angular momentum ℓ. This effect might conceivably induce an inversion in the ground and first excited states in ^{22}Al relative to ^{22}F, if the first excited state in ^{22}F is indeed a 3^+ state. In other words, the ground state of ^{22}Al could be a 3^+ state regardless of the ground state of ^{22}F possibly being a 4^+ state.

We report the first observation of β-delayed α emission from the ^{22}Al ground state, proceeding via the IAS in ^{22}Mg to the ground state of ^{18}Ne. As detailed below, this observation (1) uniquely determines the spin and parity of the ^{22}Al ground state to be 4^+, (2) resolves the long-standing ambiguity in the $A = 22$ isospin quintet and (3) challenges the status of ^{22}Al as a halo nucleus.

The relevant decay scheme is presented in Fig. 1. Previous studies at GANIL [23,24] and HIRFL [25] identified the β-delayed α branch to the first excited (2^+) state of ^{18}Ne (indicated by the blue arrow). However, the critical transition to the 0^+ ground state (indicated by the red arrow) remained unobserved in these experiments, likely due to the overwhelming background from β-delayed protons.

The present measurement was performed at the Facility for Rare Isotope Beams (FRIB). A 5 kW primary beam of ^{36}Ar was accelerated to 210 MeV/u before impinging on a 8.07 mm carbon production target. The resulting in-flight cocktail beam was momentum-to-charge-separated in the Advanced Rare Isotope Separator (ARIS) [28,29], reducing the beam energy to 106 MeV/u. Subsequently, the beam was guided to the Gas Stopping Area for further momentum compression, thermalization and purification. A pure, low-energy 30 keV beam of ^{22}Al was extracted from the Advanced Cryogenic Gas Stopper (ACGS) [30,31] and implanted into a thin carbon foil surrounded by a compact array of silicon detector telescopes. Just outside of the vacuum chamber, containing the silicon detector telescopes, were two high-purity germanium detectors from the LIBRA setup [32], flanking the chamber.

The low beam energy and the use of thin (60–70 μm) ΔE detectors allowed the dominant high-energy protons above 2–3 MeV to punch through the thin detectors, depositing only a fraction of their energy, while fully stopping α particles up to ∼9 MeV [33]. This suppression of the proton background, crucial for isolating the rare α decay channels, was made possible by the characteristics of the low energy beams extracted from the ACGS. The implantation rate at the setup is estimated to be around 5–10 particles per second based on the number of observed β-delayed protons throughout the experiment, correcting for the branching ratio 54.5(25) % [24] and the solid angle coverage of roughly 7% per silicon detector telescope.

The upper panel of Fig. 2 displays the energy spectrum of α particles stopped in the ΔE detectors. Two distinct peaks associated with the decay of ^{22}Al are visible above the background. The background arises from long-lived calibration sources implanted prior to the experiment. The peak at 3.29 MeV (α_1) corresponds to the previously known transition to the ^{18}Ne(2^+) state. The newly observed peak at 4.83 MeV (α_0) corresponds to the transition to the ^{18}Ne(0^+) ground state.

The identification is supported by coincidence measurements. The lower panel of Fig. 2 shows ^{18}Ne-α coincidences demonstrating the detection of low-energy signals from the opposing silicon detectors, corresponding to ^{18}Ne nuclei recoiling with the expected kinetic energies of 1.07 and 0.73 MeV for the ground and excited state transitions, respectively. We emphasize that the pure, low-energy beam extracted from the ACGS enabled the measurement of the low-energy ^{18}Ne recoils. Furthermore, a gate on the 1.887 MeV γ-ray line (the $2^+ \rightarrow 0^+$ transition in ^{18}Ne) isolates the α_1 branch, as shown in the inset of the upper panel. The particle energies in Fig. 2 have been corrected for energy losses specific to α particles in the detector dead layers and for the pulse height defect (PHD) inherent to silicon detectors calibrated with protons. The observed broadening of the recoil energies is consistent with the broader distribution of energy losses of the heavy ions in the dead layers and with PHD uncertainties.

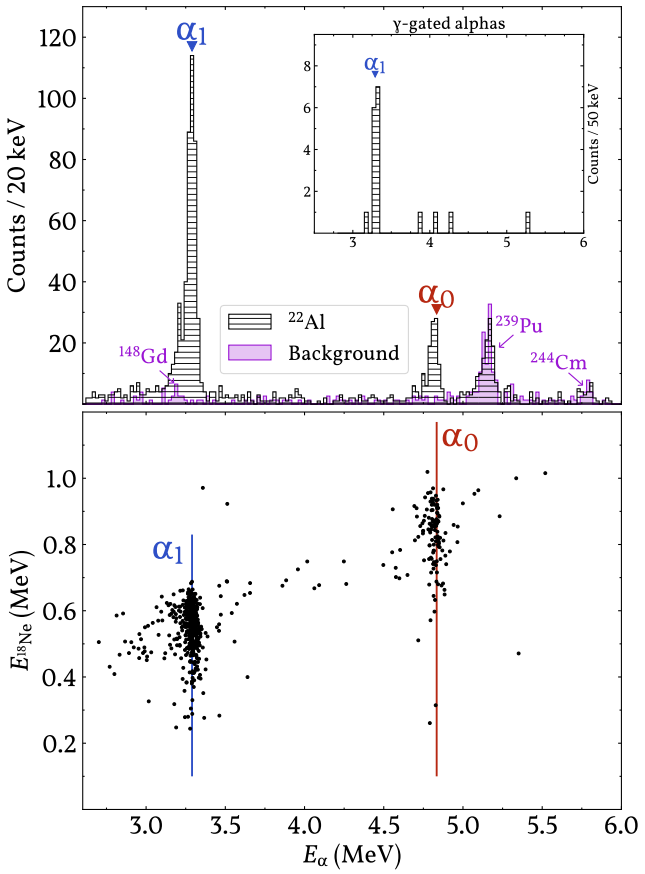

FIG. 2. Top: Singles spectrum of α-particle kinetic energies E_α, extracted from the ΔE detectors. The labels α_0 and α_1 denote transitions from the IAS in ^{22}Mg to the 0^+ ground and 2^+ first excited states of ^{18}Ne, respectively. The background spectrum (scaled from 25 h to the 33 h ^{22}Al measurement time) is dominated by preimplanted calibration sources. The inset shows coincidences with the 1.887 MeV γ transition in ^{18}Ne. Bottom: ^{18}Ne recoil energies, $E_{^{18}\mathrm{Ne}}$, in coincidence with α particles in opposing silicon detectors. The α particles are found above the proton punch through thresholds in the ΔE detectors (as in the singles spectrum), and any signal in opposing detectors is considered a recoil.

Figure 3 illustrates how the β-delayed α particles are separated from the intense background of β-delayed protons in the decay of ^{22}Al. The thin (60–70 μm) ΔE detectors completely stop protons up to the *punch through* threshold [34] for protons, $\Delta E^{\mathrm{p}}_{\mathrm{max}}$, of 2–3 MeV. Protons with initial energies above this threshold deposit only a fraction of the energy $\Delta E^{\mathrm{p}}_{\mathrm{max}}$ in the ΔE detectors, while depositing the remainder of their energies in the thicker, backing E detectors. The relevant energies of the α particles are higher than $\Delta E^{\mathrm{p}}_{\mathrm{max}}$, but not so high that the α particles punch through the thin ΔE detectors. This enables their observation in a proton-free energy region of the thin ΔE

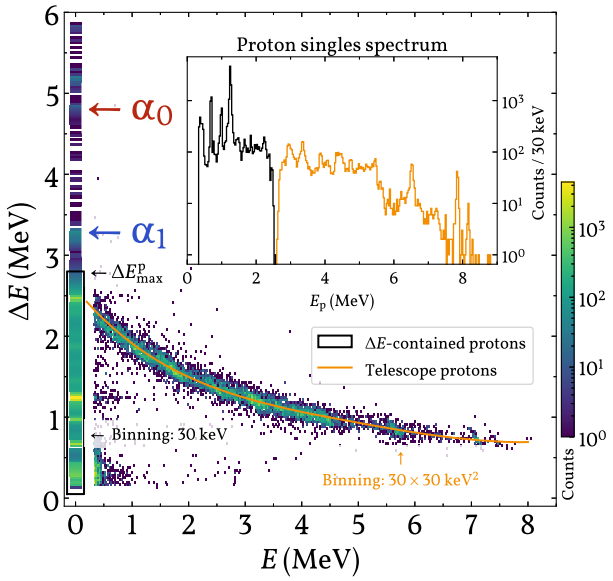

FIG. 3. Energy deposit in the ΔE detector vs energy deposit in the E detector of one of the silicon detector telescopes. Sufficiently energetic protons punch through the ΔE detector and are stopped in the E detector, generating *telescope proton events*. Events with energy deposition only in the ΔE detector without any corresponding energy deposition in the E detector, generating ΔE*-contained proton events*, are drawn with a width of 200 keV along the E axis, centered at $E = 0$. The observed β-delayed α particles in the ΔE detector, α_0 and α_1 from Fig. 2, are indicated. The indicated ΔE^{p}_{max} is the maximum energy a proton can deposit in the ΔE detector. The inset of the figure shows the reconstructed proton energies E_p from both the ΔE-contained proton events and the telescope proton events. The region in the inset where the number of ΔE-contained proton events go to zero from below and the number of telescope proton events go to zero from above is instrumental: It is due to the inherent *dead zone* of the detector telescope; see [34].

detectors. Note how the observed α particle energies would be overwhelmed by the proton energy spectrum, shown in the inset of Fig. 3, had they not been separated from the dominant proton background by use of thin ΔE detectors.

The new observation of the α_0 branch allows for a definitive assignment of the ^{22}Al ground state spin and parity: The emission of an α particle to a 0^+ state requires, by conservation of angular momentum and parity, that the parent state has natural parity and $J^\pi = \ell^\pi$. Since the IAS in ^{22}Mg is populated via superallowed Fermi decay, it shares the spin and parity of the ^{22}Al ground state. A $J^\pi = 3^+$ assignment would require $\ell = 3$ for decay to a 0^+ daughter, which implies negative parity, leading to a violation of parity conservation. Therefore, the observation of the α_0 branch mandates that the IAS—and consequently the ground state of ^{22}Al—is 4^+.

The newly determined proton separation energy of ^{22}Al, $S_p = 100.3(8)$ keV [11,12], is exceptionally low and comparable to the archetype proton halo nucleus ^{8}B [35,36] with $S_p = 136(1)$ keV. This proximity to the drip line has fueled speculation that ^{22}Al might exhibit a proton halo. However, halo formation is not determined solely by binding energy; it requires a structural configuration that allows the valence nucleon to tunnel through the confining potentials.

If the ground state of ^{22}Al were 3^+, the valence proton could occupy an $s_{1/2}$ ($\ell = 0$) orbital coupled to the ^{21}Mg$(5/2^+)$ core ground state. Lacking a centrifugal barrier, such a configuration would favor the formation of an extended halo. In contrast, the 4^+ assignment mandates that a proton coupled to the ^{21}Mg ground state must occupy a $d_{5/2}$ ($\ell = 2$) orbital. An s-wave component in the 4^+ state is only possible via coupling to high-lying excited states of the core (e.g., $7/2^+, 9/2^+$), a configuration that is energetically suppressed.

This qualitative picture is supported by recent microscopic calculations, studying specifically the potential halo nature of ^{22}Al. Relativistic Hartree-Bogoliubov studies treating ^{22}Al as a deformed or triaxial system [6,10] indicate that even under favorable conditions, the ground state wave function is dominated ($> 90\%$) by the d-wave component. Consequently, these models predict no significant enhancement of the root-mean-square radius relative to neighboring isotopes. Furthermore, recent *ab initio* calculations [37] suggest that sizable Thomas-Ehrman shifts are ubiquitous in sd-shell mirror nuclei; these shifts can rationalize the low separation energy and level ordering in the $A = 22$ system without necessitating the spatial delocalization characteristic of a halo.

We therefore conclude that despite the vanishingly small separation energy, the 4^+ ground state of ^{22}Al is likely a standard nuclear system confined by high potential barriers. The valence proton is confined by a d-wave centrifugal barrier which, in concert with the Coulomb barrier, renders the formation of a halo highly improbable despite the vanishingly small proton separation energy. We note, however, that a subtle enhancement of the surface density or a "soft" tail in the wave function cannot be strictly excluded by spectroscopy alone. The ultimate confirmation of the compact nature of ^{22}Al awaits a measurement of its charge or matter radius.

The successful delivery of exotic nuclei at low energy from the ACGS at FRIB represents a significant advance for experimental studies near the drip lines. In this work, the pure, low-energy beams from the ACGS enabled both a sensitive particle identification technique that separated rare low-energy α particles from the dominant proton background and the detection of coincident low-energy ^{18}Ne recoils. This capability was instrumental in the first observation of the β-delayed α decay to the ground state of ^{18}Ne.

The lowest-lying known excited 1^+ state in ^{22}Al (Fig. 1) is unbound and thus cannot form a halo [6]. Should an excited 3^+ state in ^{22}Al lie below the proton separation

energy $S_p = 100.3(8)$ keV, it remains a candidate for extended structure.

Finally, while our spectroscopic result provides the angular momentum constraint deemed critical in [11], the ultimate quantification of the proton wave function's spatial extent requires a direct observable, e.g., a charge radius measurement. While interaction cross-section measurements could provide complementary evidence, laser spectroscopy of low-energy beams—now feasible in the FRIB gas stopping area—appears to be the most direct path to conclusively settle the question of the ^{22}Al radius.

Acknowledgments—The authors acknowledge the support from the Independent Research Fund Denmark, Projects No. 9040-00076B, No. 2032-00066B, and No. 4283-00172B, from the Swedish Research Council, Project No. 2022-04248, from the U.S. National Science Foundation under Grants No. PHY-1913554, No. PHY-2209429, and No. PHY-2514797, from the Spanish MICIU/AEI/10.13039/501100011033, and from FEDER, EU, under Project No. PID2022-140162NB-I00. This material is based upon work supported by the U.S. Department of Energy, Office of Science, Office of Nuclear Physics and used resources of the Facility for Rare Isotope Beams (FRIB) Operations, which is a DOE Office of Science User Facility under Award No. DE-SC0023633.

Data availability—The data that support the findings of this article are not publicly available upon publication because it is not technically feasible and/or the cost of preparing, depositing, and hosting the data would be prohibitive within the terms of this research project. The data are available from the authors upon reasonable request.

[1] B. Jonson, Light dripline nuclei, Phys. Rep. **389**, 1 (2004).
[2] K. Riisager, Nuclear halo states, Rev. Mod. Phys. **66**, 1105 (1994).
[3] A. S. Jensen, K. Riisager, D. V. Fedorov, and E. Garrido, Structure and reactions of quantum halos, Rev. Mod. Phys. **76**, 215 (2004).
[4] I. Tanihata, Neutron halo nuclei, J. Phys. G **22**, 157 (1996).
[5] C. Lehr *et al.*, Unveiling the two-proton halo character of ^{17}Ne: Exclusive measurement of quasi-free proton-knockout reactions, Phys. Lett. B **827**, 136957 (2022).
[6] K. Y. Zhang, C. Pan, and S. Wang, Examination of the evidence for a proton halo in ^{22}Al, Phys. Rev. C **110**, 014320 (2024).
[7] K. Y. Zhang and X. X. Lu, Microscopic description of the proton halo in ^{12}N, Phys. Lett. B **871**, 139989 (2025).
[8] B. A. Brown and P. G. Hansen, Proton halos in the 1*s*0*d* shell, Phys. Lett. B **381**, 391 (1996).
[9] J. Lee *et al.*, Large isospin asymmetry in ^{22}Si/^{22}O mirror Gamow-Teller transitions reveals the halo structure of ^{22}Al, Phys. Rev. Lett. **125**, 192503 (2020).
[10] P. Papakonstantinou, M. Mun, C. Pan, and K. Zhang, Proton halo structures and ^{22}Al, Phys. Rev. C **112**, 044301 (2025).
[11] S. E. Campbell, G. Bollen, B. A. Brown, A. Dockery, C. M. Ireland, K. Minamisono, D. Puentes, B. J. Rickey, R. Ringle, I. T. Yandow, K. Fossez, A. Ortiz-Cortes, S. Schwarz, C. S. Sumithrarachchi, and A. C. C. Villari, Precision mass measurement of the proton dripline halo candidate ^{22}Al, Phys. Rev. Lett. **132**, 152501 (2024).
[12] M. Z. Sun *et al.*, Ground-state mass of ^{22}Al and test of state-of-the-art ab initio calculations, Chin. Phys. C **48**, 034002 (2024).
[13] The proton separation energy $S_p = 100.3(8)$ keV of ^{22}Al is the weighted average of 100.4(8) keV from [11] and 90 (10) keV from [12].
[14] B. Blank and M. J. G. Borge, Nuclear structure at the proton drip line: Advances with nuclear decay studies, Prog. Part. Nucl. Phys. **60**, 403 (2008).
[15] M. D. Cable, J. Honkanen, R. F. Parry, H. M. Thierens, J. M. Wouters, Z. Y. Zhou, and J. Cerny, Beta-delayed proton decay of an odd-odd $T_z = -2$ isotope, ^{22}Al, Phys. Rev. C **26**, 1778 (1982).
[16] M. D. Cable, J. Honkanen, R. F. Parry, S. H. Zhou, Z. Y. Zhou, and J. Cerny, Discovery of beta-delayed two-proton radioactivity: ^{22}Al, Phys. Rev. Lett. **50**, 404 (1983).
[17] B. A. Brown, Isospin-forbidden β-delayed proton emission, Phys. Rev. Lett. **65**, 2753 (1990).
[18] M. S. Basunia, Nuclear data sheets for A = 22, Nucl. Data Sheets **127**, 69 (2015).
[19] C. N. Davids, D. R. Goosman, D. E. Alburger, A. Gallmann, G. Guillaume, D. H. Wilkinson, and W. A. Lanford, β decay of ^{22}F, Phys. Rev. C **9**, 216 (1974).
[20] S. Lee, S. L. Tabor, A. Volya, A. Aguilar, P. C. Bender, T. A. Hinners, C. R. Hoffman, M. Perry, and V. Tripathi, Electromagnetic transitions in neutron-rich ^{22}F, Phys. Rev. C **76**, 034308 (2007).
[21] J. Chen *et al.*, Experimental study of the effective nucleon-nucleon interaction using the ^{21}F(d, p)^{22}F reaction, Phys. Rev. C **98**, 014325 (2018).
[22] B. A. Brown and W. A. Richter, New "USD" Hamiltonians for the *sd* shell, Phys. Rev. C **74**, 034315 (2006).
[23] B. Blank, F. Boué, S. Andriamonje, S. Czajkowski, R. Del Moral, J. P. Dufour, A. Fleury, P. Pourre, M. S. Pravikoff, N. A. Orr, K.-H. Schmidt, and E. Hanelt, The spectroscopy of ^{22}Al: A βp, β2p and $\beta\alpha$ emitter, Nucl. Phys. **A615**, 52 (1997).
[24] N. L. Achouri, F. de Oliveira Santos, M. Lewitowicz, B. Blank, J. Äystö, G. Canchel, S. Czajkowski, P. Dendooven, A. Emsallem, J. Giovinazzo, N. Guillet, A. Jokinen, A. M. Laird, C. Longour, K. Peräjärvi, N. Smirnova, M. Stanoiu, and J.-C. Thomas, The β-decay of ^{22}Al, Eur. Phys. J. A **27**, 287 (2006).
[25] C. G. Wu *et al.*, β-decay spectroscopy of the proton drip-line nucleus ^{22}Al, Phys. Rev. C **104**, 044311 (2021).
[26] D. R. Tilley, H. R. Weller, C. M. Cheves, and R. M. Chasteler, Energy levels of light nuclei A = 18–19, Nucl. Phys. **A595**, 1 (1995).
[27] R. B. Firestone, Nuclear data sheets for A = 21, Nucl. Data Sheets **127**, 1 (2015).
[28] M. Portillo, B. M. Sherrill, Y. Choi, M. Cortesi, K. Fukushima, M. Hausmann, E. Kwan, S. Lidia, P. N. Ostroumov, R. Ringle, M. K. Smith, M. Steiner, O. B. Tarasov, A. C. C. Villari, and T. Zhang, Commissioning

of the advanced rare isotope separator ARIS at FRIB, Nucl. Instrum. Methods Phys. Res., Sect. B **540**, 151 (2023).
[29] K. Fukushima, M. Cortesi, M. Hausmann, E. Kwan, P. N. Ostroumov, M. Portillo, B. M. Sherrill, M. Smith, M. Steiner, and T. Zhang, Simulation studies for beam commissioning at FRIB advanced rare isotope separator, Nucl. Instrum. Methods Phys. Res., Sect. B **541**, 53 (2023).
[30] K. R. Lund, G. Bollen, D. Lawton, D. J. Morrissey, J. Ottarson, R. Ringle, S. Schwarz, C. S. Sumithrarachchi, A. C. C. Villari, and J. Yurkon, Online tests of the advanced cryogenic gas stopper at NSCL, Nucl. Instrum. Methods Phys. Res., Sect. B **463**, 378 (2020).
[31] R. Ringle, G. Bollen, K. Lund, C. Nicoloff, S. Schwarz, C. S. Sumithrarachchi, and A. C. C. Villari, Particle-in-cell techniques for the study of space charge effects in the advanced cryogenic gas stopper, Nucl. Instrum. Methods Phys. Res., Sect. B **496**, 61 (2021).
[32] L. J. Sun, J. Dopfer, A. Adams, C. Wrede, A. Banerjee, B. A. Brown, J. Chen, E. A. M. Jensen, R. Mahajan, T. Rauscher, C. Sumithrarachchi, L. E. Weghorn, D. Weisshaar, and T. Wheeler, Extension of the particle x-ray coincidence technique: The lifetimes and branching ratios apparatus, Phys. Rev. C **111**, 055806 (2025).
[33] J. F. Ziegler, M. D. Ziegler, and J. P. Biersack, SRIM—the stopping and range of ions in matter (2010), Nucl. Instrum. Methods Phys. Res., Sect. B **268**, 1818 (2010).
[34] E. A. M. Jensen, K. Riisager, and H. O. U. Fynbo, Extracting clean low-energy spectra from silicon strip detector telescopes around punch through energies, Nucl. Instrum. Methods Phys. Res., Sect. A **1055**, 168531 (2023).
[35] M. H. Smedberg *et al.*, New results on the halo structure of ^{8}B, Phys. Lett. B **452**, 1 (1999).
[36] G. A. Korolev *et al.*, Halo structure of ^{8}B determined from intermediate energy proton elastic scattering in inverse kinematics, Phys. Lett. B **780**, 200 (2018).
[37] H. H. Li, Q. Yuan, J. G. Li, M. R. Xie, S. Zhang, Y. H. Zhang, X. X. Xu, N. Michel, F. R. Xu, and W. Zuo, Investigation of isospin-symmetry breaking in mirror energy difference and nuclear mass with ab initio calculations, Phys. Rev. C **107**, 014302 (2023).